Available online at www.sciencedirect.com
ScienceDirect
Journal of Magnetic Resonance 182 (2006) 229–238
JMR Journal of Magnetic Resonance
www.elsevier.com/locate/jmr

Ultra-stable temperature control in EPR experiments: Thermodynamics of gel-to-liquid phase transition in spin-labeled phospholipid bilayers and bilayer perturbations by spin labels

Ali M. Alaouie, Alex I. Smirnov *

Department of Chemistry, North Carolina State University, 2620 Yarbrough Drive, Box 8204, Raleigh, NC 27695-8204, USA

Received 15 March 2006; revised 25 June 2006
Available online 21 July 2006

Abstract

An ultra-stable variable temperature accessory for EPR experiments with biological samples has been designed and tested. The accessory is comprised from a digitally controlled circulator bath that pumps fluid through high-efficiency aluminum radiators attached to an EPR resonator of a commercial X-band EPR spectrometer. Temperature stability of this new accessory after a 15 min re-equilibration is at least ±0.007 K. For a standard 1-cm-long capillary sample arranged inside an EPR tube filled with silicon oil, the temperature variations do not exceed ±0.033 K over the sample temperature range from 283 to 333 K. This new accessory has been tested by carrying out a comparative spin-labeling EPR and differential scanning calorimetry (DSC) study of the gel-to-liquid phase transition in multilamellar vesicles (MLV) composed of a synthetic phospholipid 1,2-dimyristoyl-*sn*-glycero-3-phosphatidylcholine (DMPC). We demonstrate that the gel-to-liquid phase transition temperatures of MLV DMPC measured by EPR and DSC agree within ±0.02 K experimental error even though the sample for EPR study was labeled with 1 mol% of 5PC (1-palmitoyl-2-stearoyl-(5-doxyl)-*sn*-glycero-3 phosphocholine). Cooperative unit number measured by EPR, $N = 676 \pm 36$, was almost 50% higher than that obtained from DSC ($N = 458 \pm 18$). These high values of N indicate that (i) the lipid domains should include at least several spin-labeled lipid molecules and (ii) the spin-probe 5PC molecules are not excluded into domains that are different from the bulk lipid phase as was speculated earlier. Overall, our data provide DSC and EPR evidence that in studies of the gel-to-liquid phase transition, the effect of bilayer perturbation by spin-labeled lipids is negligible and therefore thermodynamic parameters of the phase transition can be accurately measured by spin-labeling EPR. This might serve as an indication when spin-labeled molecules with structures similar to those of lipids are introduced at low concentrations, they are easily accommodated by fluid phospholipid bilayers without significant losses of the lipid cooperativity.

Keywords: Lipid bilayer; Phase transition; Variable temperature accessory; Cooperativity

1. Introduction

Sample temperature control in commercial EPR spectrometers is typically achieved using a gas flow system. In such a setup, a gas (typically nitrogen) is passed through a heater and/or a heat exchanger and is subsequently flown to the cavity or directly to the sample. Variable temperature (VT) accessories for commercial X-band EPR experiments provided by either Varian (Palo Alto, CA) in the past or currently by a Bruker Biospin (Billerica, MA) have both the heater and the temperature sensor located before the gas enters a vacuum-insulated dewar that directs the gas through EPR resonator. Although with a proper care, such as by stabilizing the gas flow and fixing sample position in the dewar insert, the sample temperature stability could be improved, it rarely exceeds ±0.1 K [1]. Furthermore, several authors noted that inevitable temperature gradients existing in the dewar insert result in 0.5–2.0 K

* Corresponding author. Fax: +1 919 513 7353.
E-mail address: Alex_Smirnov@ncsu.edu (A.I. Smirnov).

1090-7807/$ - see front matter © 2006 Elsevier Inc. All rights reserved.
doi:10.1016/j.jmr.2006.07.002

errors in sample temperature readings even if the experimental temperature only slightly differs from the ambient [1,2].

Temperature gradients of ca. 0.5 K/sample and temperature errors/instabilities of ±0.1 K or even ±0.5 K are routinely neglected in many EPR experiments. However, such experimental uncertainties may be unacceptable for variable temperature EPR studies of biological samples especially when considering the gel-to-liquid phase transition of multilamellar vesicles from synthetic phosphatidylcholines that is known to occur over a narrow (ca. 0.1–0.5 K) temperature range as a highly cooperative molecular rearrangement [3].

One simple way to decrease temperature gradients in EPR experiments with aqueous biological samples is to place the sample capillary into a standard EPR quartz tube filled with silicon oil for temperature stabilization [4]. Morse and co-workers extended this approach by directly controlling the oil temperature with a circulator bath [2]. In their setup, silicon oil was circulated through a dewar directly placed into an EPR cavity. While these authors managed to decrease the sample's temperature gradients to as low as 0.01 K cm^{-1}, uncertainty in the sample's temperature was about 0.1 K. It should be noted here that the variable temperature system of Morse and co-workers requires a specially designed evacuated quartz dewar. Although such a dewar would accommodate a standard EPR quartz tube, it would not permit a standard EPR flat cell or a Bruker AquaX accessory that are often employed in studies of aqueous samples because of superior sensitivity.

Here we describe a simple, inexpensive, and efficient VT accessory that is suitable for virtually any research-grade EPR spectrometer and is capable of providing stable and very accurate temperature readings in spin-labeling EPR studies of biological samples. The accessory is comprised of a digitally controlled circulator bath that pumps fluid through high-efficiency aluminum radiators surrounding the rectangular EPR resonator on both sides in order to maintain its temperature. This new accessory has been tested by (i) mapping the temperature in the sample region with a high-precision thermocouple and (ii) carrying out a comparative spin-labeling EPR and differential scanning calorimetry (DSC) study of the gel-to-liquid phase transition in multilamellar vesicles (MLV) composed of a synthetic phospholipid DMPC (1,2-dimyristoyl-*sn*-glycero-3-phosphatidylcholine).

Another reason for carrying out comparative EPR and DSC studies with such a high degree of accuracy was our intent to investigate a long-standing concern of bilayer perturbation by spin-labeled phospholipids. Earlier calorimetric and EPR studies have shown that lipid bilayers composed from pure spin-labeled lipids exhibit thermal behavior resembling that of phosphatidylcholines bearing double bonds or branched methyl groups at similar locations on the acyl chains [5,6]. While the nitroxide moiety is small compared with fluorescent probes that are commonly employed in membrane studies, the structure of spin-labeled phospholipids and spin-labeled steroid analogues still differs from unlabeled molecules. Depending on experimental conditions, such molecules when added to lipid bilayers could form separate domains and/or aggregate. However, many experiments have shown that for labels present in concentrations less than ca. 1 mol%, the EPR spectra exhibit no broadening from spin–spin interactions (*e.g.* [11,22]). This indicates the absence of any significant spin-label aggregation. Thus, the solution of spin-labeled lipids in the bilayer is expected to behave ideally and the EPR spectra would report the phase properties of the bulk bilayer. In the past it has been shown that the EPR spectra of membrane spin labels serve as good indicators of the bilayer phase state [7–9] and could be used to measure phase transition temperatures and the phase diagrams for binary lipid mixtures [7]. Systematic studies of the effects of various small molecules such as different spin probes and spin-labeled fatty acids on the bilayer phase properties confirmed that for spin-probe concentrations below ca. 1–1.5% no measurable broadening of the DSC curves is observed [10].

Despite these and other observations confirming that spin labels at low concentrations have little or no effect on the bulk bilayer properties, some authors expressed concerns that doxyl-labeled fatty acids and lipids increase the bilayer heterogeneity at least in the vicinity of the spin label (*e.g.*, see [10] and references therein). One of the presented arguments is that nitroxide doxyl groups cannot be tightly packed in the bilayer as the alkyl chains alone and therefore the immediate nitroxide surrounding should be somewhat more fluid than the bulk of the membrane [10]. Consequently, the melting point of the nitroxide local domain should be depressed. Then spin-labeling EPR would report systematically lower phase transition temperature than, for example, DSC. Although DSC and EPR data on the bilayer phase transition temperature were compared in several studies (*e.g.* [4,12]), the uncertainty in sample temperature during EPR measurements was typically not better than 0.5–1.0 K and, therefore, is insufficient for drawing concise conclusions. The goal of deriving cooperative unit numbers in our EPR study was to shed some light on whether a nitroxide would "... at least to some extent, manufacture its own liquid domain ..." when placed in the bilayer [11]. To summarize, it appears that a more accurate comparison of thermodynamic parameters of bilayer phase transition temperature measured by EPR and DSC is needed to resolve a long-standing question on possible bilayer perturbation by spin labels: do spin-labeled lipids report on the thermodynamic parameters of the bilayer defect sites or those of the bulk bilayer? Another motivation for this work was to demonstrate that spin-labeling EPR could be used successfully in studying systems with slow kinetics of the phase transition.

2. Experimental

2.1. Materials and sample preparation

Synthetic phospholipid DMPC (1,2-dimyristoyl-*sn*-glycero-3-phosphocholine) and spin-labeled phospholipid

5PC (1-palmitoyl-2-stearoyl-(5-doxyl)-*sn*-glycero-3-phosphocholine) were purchased from Avanti Polar Lipids (Alabaster, Alabama) in chloroform solutions and were stored in a freezer at 223 K prior to use. Spin-labeled multilamellar vesicles were prepared by mixing chloroform solutions of DMPC and 5PC in 100:1 molar ratio. Consequently, chloroform was removed by a rotary evaporator yielding a thin lipid film on the surface of a round bottom flask. Unlabeled (control) sample was prepared following the same procedure using DMPC from the same stock but no 5PC was added. Residual chloroform was removed by keeping the vials on a vacuum pump with a liquid nitrogen trap overnight. Multilamellar vesicles were formed by adding 50 mM Hepes, pH 7.0, buffer and cycling the flask for at least 10 times between liquid nitrogen and a water bath at 305 K. The final concentration of lipids in aqueous media was 200 mg ml^{-1}.

2.2. EPR and DSC measurements

X-band (9.5 GHz) EPR measurements were carried out with either a Varian Century Series E-102 spectrometer (Palo Alto, CA) or a Bruker-IBM ER200D-SRC spectrometer equipped with a variable temperature accessory ER4111VT (all from IBM Instruments, Inc., Danbury, CT). Both spectrometers were interfaced with personal computers. Aqueous dispersion of spin-labeled bilayers was drawn into a glass capillary (1.10 mm i.d., 1.50 mm o.d.; Clay Adams/Becton, Dickinson and Company, Parsippany, NJ). The capillary was sealed with a Bruker Biospin X-sealant (Billerica, MA) and inserted into standard quartz EPR tube, which was then fixed inside a TE102-type resonator.

Sample temperature was measured with a VWR International (West Chester, PA) digital thermometer equipped with a microstainless steel probe. The VWR thermometer has resolution of 0.001 K and accuracy of ±0.05 K. The thermometer was calibrated using standards traceable to NIST. Although the microtemperature probe is somewhat magnetic, its diameter is only 1.3 mm. Such a thin and 7.0-cm-long probe could be easily placed just above the sample in an EPR cavity. Preliminary EPR experiments were carried out with a Fluke16 Digital Multimeter (Carrollton, TX) equipped with a Fluke 80BK integrated probe (K-type thermocouple, ±0.1 K accuracy).

DSC experiments were carried out with both spin-labeled and unlabeled DMPC. In both experiments, approximately 20 mg of aqueous lipid dispersion was placed into a steel high-volume pan. The pan was sealed with a lid and an o-ring, and loaded into a Q100 calorimeter (TA Instruments, New Castle, DE). Each sample contained approximately 4 mg of DMPC.

In order to compare EPR and DSC results, all thermometers were cross-calibrated by observing the melting point temperature, $T_m = 299.95$ K, of diphenyl ether (purchased from Alfa Aesar, Ward Hill, MA). Calibration of the Q100 calorimeter was confirmed by observing the melting of diphenyl ether in the same high-volume steel pans. For the VWR and Fluke thermometers a calibration was performed using a 1A6304 Melting Point Apparatus (Electrothermal, England). A sample of diphenyl ether was packed into a KIMAX-51 glass capillary tube (1.5–1.8 mm o.d., 0.2 mm wall thickness, 90 mm length; Kimble/Kontes, Vineland, NJ) and inserted in the central of the three sample compartments of the Melting Point Apparatus whereas the thermocouples were positioned in the adjacent compartments. Once melting of the sample was detected, temperature reading for each of the thermocouples was recorded.

3. Results and discussion

3.1. Variable temperature EPR accessory

In order to achieve temperature stability and resolution in an EPR experiment comparable to that of a DSC, we have assembled a special variable temperature accessory (Figs. 1 and 2) based on a Fisher Scientific (Hampton, New Hampshire) Isotemp Model 1016 refrigerating circulator bath. This microprocessor-controlled circulator is capable of pumping a fluid up to 3 m of a vertical pump-head. The temperature range of this bath is from 253 to 473 K with temperature stability of ±0.01 K. In our setup, tap water or an antifreeze/coolant mixture P/N AF-1100 (Advance Auto Parts, Roanoke, Virginia) from the circulator bath was directed to the aluminum radiators (Model HDC1-A01, Koolance, Inc., Federal Way, WA) that were pressed against the sides of the Varian EPR resonator so the EPR sample region was positioned approximately in the middle between the radiator plates (Fig. 2). The original purpose of these radiators is to capture heat from high-performance IDE and/or SCSI computer drives. The

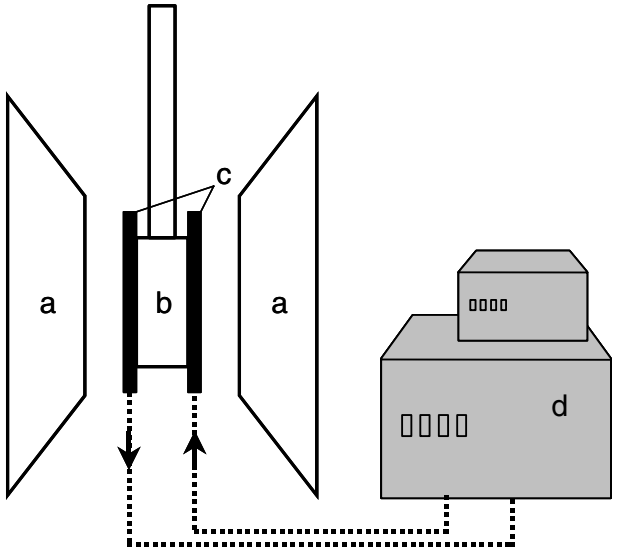

Fig. 1. Schematic drawing of a variable temperature accessory described in the text: (a) electromagnet poles; (b) EPR resonator; (c) aluminum radiators; (d) digital refrigerating circulator bath.

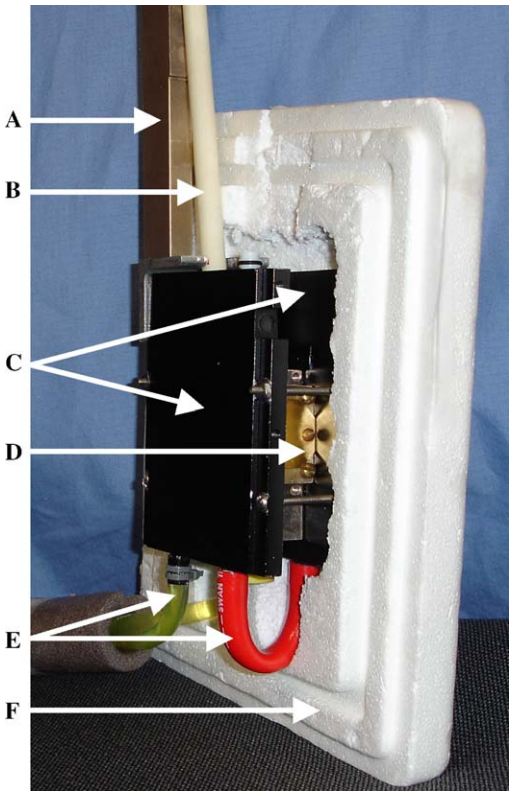

Fig. 2. Photograph of the NCSU VT probehead assembly for a Varian X-band TE_{102}-type resonator with a half of the Styrofoam™ insulation removed: (A) X-band waveguide, (B) iris tuning rod, (C) aluminum radiators, (D) front plate of the EPR resonator, (E) connecting tubing for heating/cooling fluid, (F) one of the two Styrofoam™ insulating enclosures.

radiators are nonmagnetic—according to the manufacturer they are made from anodized aluminum to resist corrosion. Additionally, since the radiators weight only 340.2 g each and have dimensions of $10.2 \times 14.0 \times 1.1$ cm, they can easily be incorporated into the gap between the resonator and the magnet poles of many commercial EPR spectrometers. In our experiments, the EPR resonator was sandwiched between the radiators that were bolted together through the available mounting holes.

In the North Carolina State University (NCSU) VT accessory, the temperature could be controlled with either an internal Fisher Isoterm bath temperature sensor or an external sensor that could be attached, for example, to the sample. In our experiments the internal sensor was utilized and the actual temperature of the sample or near the sample region was measured using the VWR thermometer.

For a series of temperature gradient measurements, the circulator bath temperature was set to a target temperature that varied from 283 to 333 K. The room temperature was about 298.5 K. Following the procedure of Ref. [4], the sample capillary was inserted into a standard 3×4 mm EPR quartz tube that was filled with a silicon oil to about 5 cm height and consequently centered in the EPR cavity. The VWR microtemperature probe was positioned in the center of the tube and moved with vertical steps of 0.5 cm. During these calibration measurements, the EPR spectrometers were switched off to avoid any microwave and/or Eddy current heating of the temperature probe. Results of these measurements are summarized in Fig. 3.

Fig. 3A shows a set of initial measurements in which the surface of radiators was left uninsulated. When the EPR tube temperature was maintained at 306.5 K (about 8 K higher than the temperature in the lab), the temperature gradient was only 0.016 ± 0.001 K cm^{-1} (Fig. 3A, open circles); however, the gradient increased to 0.050 ± 0.001 K cm^{-1} while the tube temperature was increased to 316.3 K (Fig. 3A, filled squares). Note, that in a TE_{102}-type X-band EPR resonator, the EPR intensity drops rapidly when the sample is moved outside the central 1 cm region [13]. Thus, for a 1-cm-long sample in this arrangement, the uncertainty in temperature does not exceed ± 0.025 K, which is sufficient for many experiments

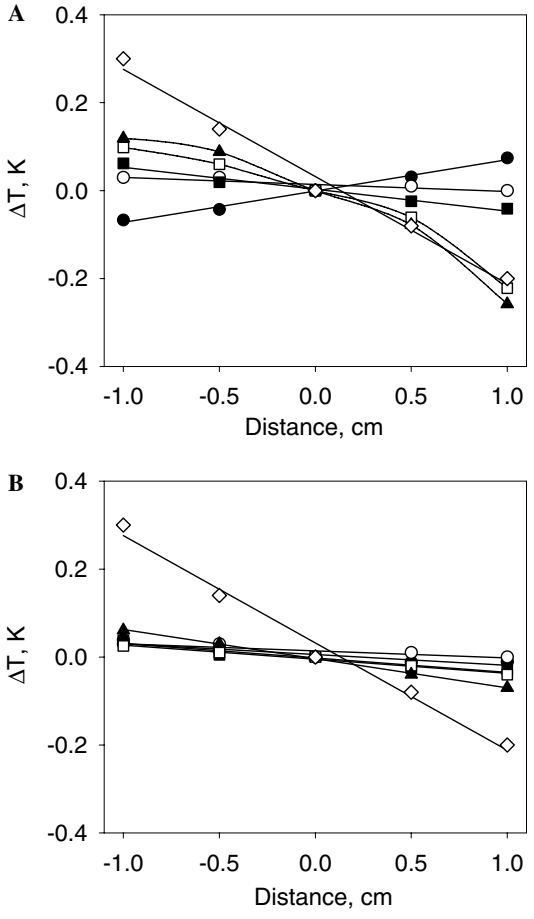

Fig. 3. Variation in temperature along a standard (i.d. = 3 mm, o.d. = 4 mm) quartz EPR tube filled with silicon oil for an uninsulated (A) and (B) Styrofoam™-insulated configurations of the NCSU variable temperature accessory and various bath target temperatures: (○) 283 K, (●) 306 K, (□) 313 K, (■) 323 K, and (▲) 333 K. The distance was measured from the center of the cavity and is positive above the center. For a comparison, the temperature gradient along the same EPR sample tube inside the Bruker-IBM variable temperature accessory that was set to 307 K is shown as (◇) in both (A) and (B). Magnitudes of the temperature gradients are discussed in the text.

with phospholipid bilayers in the range from room temperature to 316 K. These gradients increased as the set temperature deviated further from the ambient conditions. For example, at 332 K, the highest temperature tested (about 33 K above room temperature), the gradient within the central 1 cm of the cavity was still only 0.166 ± 0.002 K cm^{-1} but increased up to 0.36 ± 0.01 K cm^{-1} once the sensor was moved out of this region (Fig. 3A).

It was also observed that the temperature in the middle of the sample deviated from the internal temperature of the circulator bath. This deviation is associated with thermal losses through 3/8 in. i.d. thick-wall. Tygon tubing (purchased from Fisher Scientific, Hampton, New Hampshire) connecting the bath with the radiators as well with losses from the radiator surfaces. In order to decrease these losses and further suppress temperature gradients we have insulated the radiator and other exposed surfaces by encapsulating the entire probehead including the radiators into a simple Styrofoam™ (extruded polystyrene insulation, The Dow Chemical Company, Washington, DC) enclosure (Fig. 2). Using this insulated probehead we have repeated the temperature gradient experiments and found that the gradients were significantly suppressed over a larger area (Fig. 3B). Specifically, over the entire temperature range tested (from 283 to 333 K) the temperature gradient within the central 2 cm region of the cavity did not exceed 0.066 ± 0.001 K cm^{-1} (Fig. 3B).

One could argue that in our VT accessory the largest heat sink in the system is the waveguide attached to the back of the EPR resonator. Thus, we have also measured temperature gradients perpendicular to the long axis of the EPR tube in our VT accessory. For example, for an uninsulated setup with a resonator temperature of 322.3 K the perpendicular gradient was only 0.034 ± 0.001 K cm^{-1} vs. a vertical gradient of 0.121 ± 0.001 K cm^{-1} for the same configuration. It should be noted here that the internal diameter of a typical sample for X-band EPR rarely exceeds 3 mm and the preferred configuration of aqueous and tissue cells is such that the sample thickness in the direction of the perpendicular gradient rarely exceeds 1 mm. Thus, we concluded that the perpendicular gradient is insignificant in our system and the vertical gradient is the major source of error. This should not be surprising because the radiators employed in NCSU VT extend over the entire EPR resonator surfaces (Fig. 3). We have also found that centering the resonator with respect to the radiators is critical in suppressing vertical temperature gradients.

Fig. 4 summarizes the maximum variation in the sample temperature over the central 1 cm region of the EPR resonator as a function of the sample temperature offset from ambient conditions. The temperature variations show approximately linear trends with the offset temperature for both insulated and uninsulated configurations of the NCSU VT. Fig. 4 further demonstrates a clear advantage of the Styrofoam™ insulation in suppressing temperature gradients.

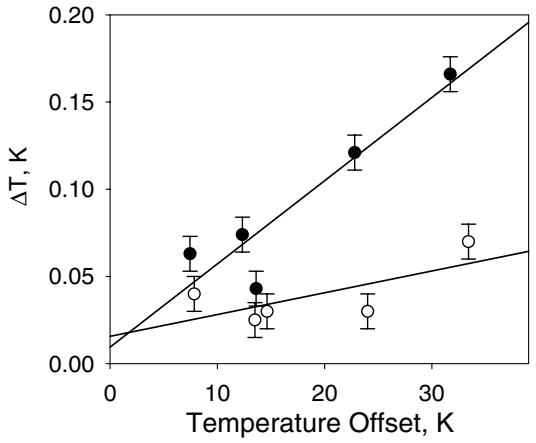

Fig. 4. The maximum variations in the sample temperature, ΔT, measured over the central 1 cm region of the EPR resonator as a function of the sample temperature offset from the ambient conditions: (●) corresponds to the uninsulated and (○) to the insulated configuration of the NCSU variable temperature accessory.

For comparison, the temperature gradient along the same EPR tube filled with silicon oil was measured for a commercial Bruker-IBM VT accessory ER4111VT (Figs. 3A and B, open diamonds). In this arrangement, the EPR sample tube was placed inside a special quartz Dewar that was kept under a constant flow of a heat-exchanging gas. In our experiments, the nitrogen flow rate was 1.9 m^2 min^{-1} and the temperature was set equally to 307 K, which was only 10 K above the ambient temperature on the day of the experiment. From linear regression the temperature gradient inside the oil-filled EPR tube when used with the Bruker-IBM VT was 0.27 ± 0.01 K cm^{-1}, which constitutes at least fivefold increase when compared with the NCSU VT in the uninsulated configuration under conditions when the sample temperature in both VTs is approximately the same.

We have also studied deviation of the sample temperature from the bath set temperature. Fig. 5 shows plots of

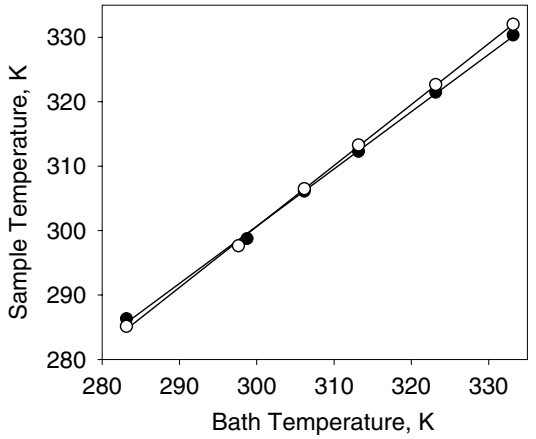

Fig. 5. Sample vs. bath temperature calibration for an uninsulated (●) and insulated (○) configurations of the NCSU variable temperature accessory.

the sample temperature in the middle of the cavity vs. set temperature of the bath for the uninsulated (filled circles) and the insulated (open circles) configuration. As one would expect, the slope for the insulated configuration (0.964 ± 0.001) exceeds that for the uninsulated setup (0.946 ± 0.001). Note, that the VWR thermometer and the bath sensor were not cross-calibrated and therefore some temperature offset is expected.

In order to ensure that the thermodynamic parameters measured by EPR are comparable with those obtained from DSC experiments that are carried out by heating or cooling the sample at a constant rate, it is highly desirable to avoid any significant oscillations in temperature of the sample when approaching the target value. One reason for such a concern stems from the fact that the phase properties of lipid bilayers are known to exhibit hysteresis effects [14,15]. Therefore, even if the oscillations in temperature are unavoidable, it is desirable for the oscillations' magnitude to be less than the width of the phase transition. Accordingly, the NCSU VT accessory was tested for temperature oscillation effects. Fig. 6 shows the time course of the sample temperature after the target value of the NCSU VT was increased by 1 K. This experiment demonstrates that the temperature equilibration time of the NCSU VT is about 15 min and standard deviation of the sample temperature after that is about 0.007 K (68% confidence interval). Clearly, our VT provides temperature resolution and stability down to at least ±0.02 K and therefore is suitable for phase transitions studies of MLV that are known to occur within the 0.1–0.3 K temperature range.

3.2. Mid-point temperature and cooperativity of the MLV DMPC gel-to-liquid phase transition as measured by spin-labeling EPR

Gel-to-liquid phase transition of multilamellar DMPC bilayers was monitored from the changes in the outer nitrogen hyperfine splitting (*i.e.*, $2A_{II}$ in Fig. 7) of 5PC. Upon

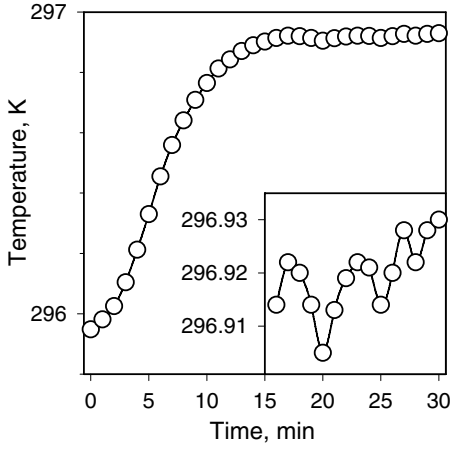

Fig. 6. Variation of the sample temperature as a function of time after the target temperature in the NCSU VT was increased by 1 K. Inset shows details of the temperature variations after the initial 15 min.

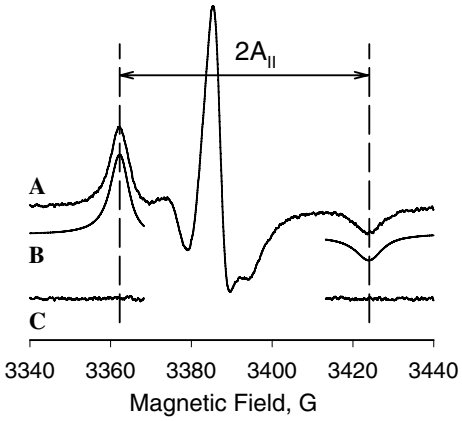

Fig. 7. (A) X-band EPR spectrum of DMPC/5PC for the bilayer in the gel phase ($T = 289.15$ K). (B) Best fit of the outer nitrogen hyperfine peaks to the Voigt line shape model. (C) Residual of the fit—a difference between the experimental (A) and the simulated (B) spectra.

melting of the phospholipid chain, changes in local dynamics of the nitroxide moiety attached to the lipid at position 5 of the acyl chain (5PC) result in a decrease in $2A_{II}$ from ca. 59 to 53 G (*e.g.* [8]) providing a convenient and reliable way of monitoring the transformation between the phospholipid phase. Our measurements of $2A_{II}$ were carried out by least-square fitting of the outer nitrogen hyperfine peaks to Voigt functions (convolutions of Gaussian and Lorentzian shapes) using software described previously [16,17]. The fitting is illustrated in Fig. 7 on an example of a DMPC/5PC EPR spectrum at 289.15 K (gel phase). The residual of the fit (Fig. 7C) shows no deviations between the fit (Fig. 7B) and the experiment (Fig. 7A) thus confirming the applicability of this model. During least-squares Levenberg–Marquardt optimization, all parameters of the Voigt functions in addition to the baseline were adjusted independently. The fitting was carried out in an automatic sequential mode, in which the best-fit parameters of a particular EPR spectrum were taken as the first approximation for the next spectrum in the temperature sequence.

DMPC/5PC EPR spectra were measured by heating the sample in 0.06–0.5 K steps with the NCSU VT. As the temperature was approaching the bilayer melting point, steps of only 0.06–0.10 K were employed whereas larger increments were used outside this region. After each step, the sample temperature was allowed to equilibrate to ±0.01 K. Fig. 8 summarizes temperature dependence of the outer nitrogen hyperfine splitting $2A_{II}$ (open circles).

We have also monitored the same DMPC phase transition experiment with a Bruker-IBM VT. While the front panel of this VT accessory allows one to dial-in the temperature with increments of 0.1 K, in a typical EPR experiment the temperature stability of the bilayer sample was not better than ±(0.1–0.2) K and the long-term temperature drift was as large as 0.5 K. Although we attempted to optimize the operation of this VT by changing the rate of the heat-exchange gas, we failed to avoid overheating

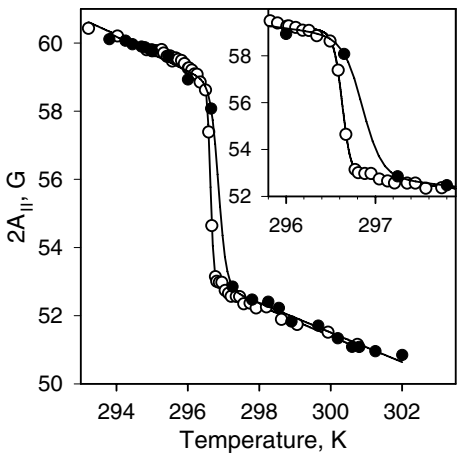

Fig. 8. Outer nitrogen hyperfine splitting, $2A_{II}$, of MLV DMPC/5PC X-band EPR spectra as a function of temperature. EPR spectra were measured with the NCSU VT (open circles) and also with the Bruker-IBM VT (filled circles). The results of the least-squares fitting of these data to a van't Hoff phase transition model are shown as solid lines. See text and Table 1 for further details. Detailed data in the vicinity of the gel-to-liquid phase transition are shown in the inset.

the bilayer sample by ca. 0.5 K and, in many cases, observed temperature oscillations up to ±0.5 K before equilibrium was reached. Nevertheless, best efforts were put forward to carefully carry out bilayer phase transition experiment with the smallest temperature steps and with as stable temperature during data acquisition as possible (*i.e.*, ±0.1 K) or until no changes in the EPR spectra are observed. The spectra were least-squares simulated as described above and the resulting outer nitrogen hyperfine splitting $2A_{II}$ were plotted as a function of temperature (Fig. 8, filled circles).

3.3. Analysis of lipid bilayer phase transition observed by EPR

For any phase transition that occur between two phases, A and B, the temperature dependence of the equilibrium constant K could be described by the van't Hoff equation:

$$K(T) = \exp\left(-\frac{\Delta H_{\mathrm{vH}}}{RT}\left(1-\frac{T}{T_{\mathrm{m}}}\right)\right) = \frac{a_{\mathrm{B}}}{a_{\mathrm{A}}}, \tag{1}$$

where ΔH_{vH} is the van't Hoff enthalpy. From this equation:

$$\left(\frac{\partial \ln K}{\partial T}\right)_p = \frac{\Delta H_{\mathrm{vH}}}{RT^2}, \tag{2}$$

where T_{m} is the mid-point temperature of the phase transition and a_{A} and a_{B} are the activities of phases A and B, respectively.

In our experiments we assumed that the activities are proportional to the fraction of spin-labeled phospholipid in a particular phase and that the outer hyperfine splitting $2A_{II}$ observed in our experiment is the weighted average of $2A_{II,\mathrm{A}}$ and $2A_{II,\mathrm{B}}$ of the coexisting phases. Temperature dependences of $2A_{II}$ corresponding to individual phases were approximated by linear functions:

$$2A_{II}(T) = 2A_{II}(T_0) + b\cdot(T-T_0), \tag{3}$$

where b is an empirical temperature coefficient. Then the temperature dependence of the outer hyperfine splitting $2A_{II}$ for the phase transition A → B is given by:

$$2A_{II}(T) = (2A_{II,\mathrm{A}}(T_0) + b_{\mathrm{A}}\cdot(T-T_0))\cdot(1-\alpha) + (2A_{II,\mathrm{B}}(T_0) + b_{\mathrm{B}}\cdot(T-T_0))\cdot\alpha, \tag{4}$$

where α is the fraction of the system in phase B:

$$\alpha = \frac{1}{1+1/K(T)}. \tag{5}$$

Eqs. (1)–(5) were employed to fit experimental data for $2A_{II}$ vs. T in order to derive the phase transition temperature, T_{m}, and the van't Hoff enthalpy, ΔH_{vH}. The best fits for the two data sets are shown as solid lines in Fig. 8 and the corresponding parameters are given in Table 1.

Fig. 8 shows that at almost all temperature readings the nitrogen hyperfine parameters $2A_{II}$ derived from the two data sets are essentially the same as it should be for identical samples. However, the least-squares fits to Eqs. (1)–(5) deviate clearly in the phase transition region because of the insufficient temperature resolution of the Bruker-IBM VT (Fig. 8, inset). Data obtained with the NCSU VT demonstrate that the gel-to-liquid phase transition in MLV DMPC/5PC occurs within a relatively narrow temperature interval (≈0.25 K) and the associated van't Hoff enthalpy is $\Delta H_{\mathrm{vH}} = (15.2\pm0.8)\times10^3$ kJ mol^{-1}. Clearly, the temperature resolution of at least 0.05–0.1 K is required to obtain reliable thermodynamic parameters for such a narrow phase transition. By considering the calorimetric enthalpy for the gel-to-liquid phase transition of DMPC to be $\Delta H_{\mathrm{cal}} \approx 22.5$ kJ mol^{-1} [18], we estimate the cooperative unit number N by dividing ΔH_{vH} to ΔH_{cal} as $N = 676\pm36$.

Evidently, inadequate temperature resolution of the Bruker-IBM VT and, as a result, insufficient temperature sampling cause T_{m} measurements to be 0.23 ± 0.05 K higher whereas the values for the van't Hoff enthalpy and the cooperative unit number are reduced by more than half when compared with values measured with the NCSU VT (Table 1). Note, that the errors for thermodynamic parameters listed in Table 1 were estimated from the data scatter without accounting for systematic errors.

3.4. Mid-point temperature and cooperativity of the MLV DMPC gel-to-liquid phase transition measured by DSC

For comparison, we have also carried out DSC phase transition experiments using the same preparations of

Table 1
Thermodynamic parameters of MLV DMPC gel-to-liquid phase transition determined by spin-labeling EPR

	NCSU VT	Bruker-IBM VT
T_{m} (K)	296.63 ± 0.01	296.86 ± 0.05
ΔH_{vH}, (×10^{-3}) kJ mol^{-1}	15.2 ± 0.8	6.7 ± 1.4
$\Delta T_{1/2}$ (K)	0.25 ± 0.01	0.58 ± 0.12
Cooperative unit, N	676 ± 36	298 ± 62

1 mol% spin-labeled and unlabeled MLV DMPC. A series of DSC heating curves for each of the samples was measured at progressively decreasing temperature rates from 1.75 to 0.1 K min^{-1}. DSC curves were least-squares fitted to extract thermodynamic parameters and to correct for remaining rate-dependent effects [19]. Two of the fit parameters—the van't Hoff enthalpy, ΔH_{vH}, and the phase transition temperature, T_m—are plotted in Fig. 9 as a function of the temperature rate, β. T_m was found to be rate-dependent and therefore was determined by linear extrapolation to $\beta = 0$ (solid and dashed lines in Fig. 9A). From this extrapolation the phase transition temperatures for the two samples were found to be identical within the uncertainty of the experimental error: $T_m = 296.63 \pm 0.02$ and 296.62 ± 0.02 K for the control and spin-labeled MLV DMPC, respectively. Thus, the presence of 1 mol% of spin-labeled lipids has no measurable effect on the gel-to-liquid phase transition temperature of MLV DMPC. Both our T_m values agree well with $T_m = 296.74$ K reported for MLV DMPC [20], although in the latter experiments the lipid concentration was much lower, 10–20 mM, and 100 mM NaCl was added to the buffer.

The van't Hoff enthalpy for both samples at temperature rates $\beta \geqslant 0.4$ K min^{-1} were essentially identical and showed only moderate rate dependence. However, upon lowering the rate from $\beta = 0.4$ to 0.1 K min^{-1}, the apparent van't Hoff enthalpy increased about twofold and the difference between the control and spin-labeled DMPC samples became noticeable (Fig. 9B). This illustrates that the phase transition in multilamellar lipid vesicles occurs through a slow process that mandates a slow temperature ramp rate in order to maintain quasiequilibrium conditions. From linear extrapolation to $\beta = 0$ using only the data from the slowest rates, the van't Hoff enthalpy for spin-labeled DMPC was found to be somewhat lower than for the unlabeled sample ($\Delta H_{vH} = (10.3 \pm 0.2) \times 10^3$ vs. $(11.9 \pm 0.2) \times 10^3$ kJ mol^{-1}). The corresponding cooperative unit numbers are $N = 458 \pm 18$ and $N = 529 \pm 18$, respectively (Table 2).

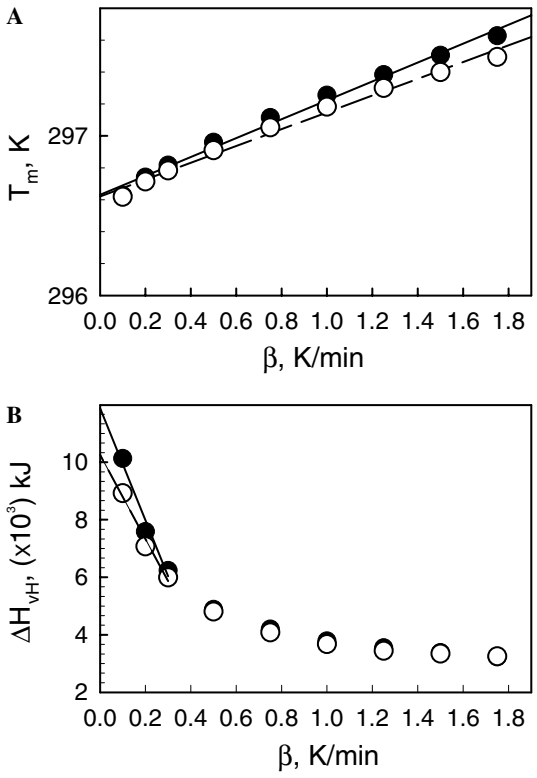

Fig. 9. Temperature (A) and van't Hoff enthalpy (B) of the gel-to-liquid phase transition of MLV DMPC determined by DSC as a function of temperature rate β: (filled circles)—control sample; (open circles)—sample doped with 1 mol% of 5PC. See text for details.

The cooperative unit number for MLV DMPC gel-to-liquid phase transition reported in literature varies from ca. $N = 330$ [16] to $N = 840$ [19]. Some of these deviations could be attributed to differences in DSC experimental conditions and whether or not the data were corrected for rate-dependent effects. In addition, it is well documented that impurities and/or other molecules partitioning in the bilayer would broaden the DSC peak and decrease the apparent cooperative unit number [3,21].

To eliminate this uncertainty in this study, all phospholipid samples employed for EPR and DSC measurements were prepared from the same batch. Thus, we speculate that a modest decrease in the van't Hoff enthalpy, ΔH_{vH}, observed for spin-labeled DMPC vs. control sample is related to the presence of spin-labeled lipids that act as impurities. However, even at 1 mol% of spin-labeled lipids, the phase transition of MLV DMPC remains highly cooperative ($N = 458 \pm 18$), confirming that under our experimental conditions 5PC has a negligible effect on the bilayer phase transition.

3.5. Comparison of EPR and DSC gel-to-liquid phase transition data for MLV DMPC bilayers

It is worthwhile to note here that in studies of gel-to-liquid bilayer phase transition EPR and DSC report on different phenomena. Specifically, the DSC signal is proportional to the heat flux to or from the sample and therefore reports on thermodynamic parameters of the entire sample. When the concentration of spin-labeled lipid is small, as in our experiments (1 mol%), one would expect an ideal solution behavior for the bulk sample and only modest changes in the bilayer thermodynamics. Indeed,

Table 2
Thermodynamic parameters of gel-to-liquid phase transition for unlabeled (control sample) MLV DMPC and DMPC doped with 1 mol% 5PC as determined by a linear extrapolation of the DSC parameters to zero temperature rate

	Control DMPC	DMPC-5PC (1 mol%)
T_m (K)	296.63 ± 0.02	296.62 ± 0.02
ΔH_{vH}, (×10^{-3}) kJ mol^{-1}	11.9 ± 0.4	10.3 ± 0.4
$\Delta T_{1/2}$ (K)	0.32 ± 0.02	0.37 ± 0.02
Cooperative unit, N	529 ± 18	458 ± 18

the DSC data presented in Table 2 are in agreement with the ideal solution model.

In contrast to DSC, EPR spectra of spin-labeled phospholipids are affected only by the local bilayer structure and report on nitroxide rotational dynamics. Line shapes of continuous wave X-band EPR spectra of ^{14}N nitroxides are sensitive to rotational correlation times shorter than $\approx 10^{-8}$ s. This time is significantly shorter than the estimated average lipid hopping time of $\approx 3 \times 10^{-7}$ s when a bilayer is in the fluid phase [22]. Thus, the time scale of X-band EPR experiment is such that it provides a snapshot of a transient molecular cage surrounding the nitroxide moiety and it is too short to allow for the lipid to exchange with the bulk. The local concentration of the nitroxide in such a cage is high and the molecular packing could be different from that of the bulk phospholipids if there is a perturbation from the nitroxide moiety. If this is the case, then thermodynamic parameters of such a cage, specifically, mid-point phase transition temperature T_m and cooperative unit number N, will be different from the rest (mostly unperturbed) bilayer.

However, comparison of the gel-to-liquid phase transition temperatures of MLV DMPC/5PC measured by spin-labeling EPR and DSC shows that T_m values agree within ± 0.02 K experimental error. Thus, we must conclude that for MLV DMPC in gel or liquid phases, the surrounding lipids should easily accommodate the presence of the doxyl ring at position 5 of the acyl chain where such rearrangement does not affect the local chain melting to any significant degree.

Comparison of the cooperative unit numbers indicates that the value computed from spin-labeling EPR study ($N = 676 \pm 36$) exceeds those measured through DSC of either spin-labeled ($N = 458 \pm 18$) or control ($N = 529 \pm 18$) samples. These numbers should be interpreted as an approximate domain size. If a nitroxide would "... manufacture its own liquid domain ..." in the bilayer as was speculated by Keith *et al.* [11], then one would expect that EPR would report a lower cooperative unit number than that observed from DSC. Our experiments indicate that this is not the case and suggest the contrary that spin-labeled lipids are not excluded into domains separated from the bulk phospholipid phase. Furthermore, if each of the spin-labeled lipids would serve as a nucleation site for growing more disordered fluid bilayer phase during the heating cycle, then the average domain size and the cooperative unit number should be about 100 for 1 mol% of 5PC. The much higher cooperative unit numbers observed in our experiments indicate that during phase transition, spin-labeled lipids behave very similar to unlabeled lipids, thus constituting ideal solution behavior. Overall, our data suggest that when similar but different molecules are present in the bilayer at low concentrations, these molecules are easily accommodated by the fluid structure of the phospholipid bilayer without any significant loss of the bilayer cooperativity.

Moreover, the cooperative unit number $N = 676 \pm 36$ observed from the EPR experiment exceeds the DSC values ($N = 458 \pm 18$ or $N = 529 \pm 18$). This is likely to be related to very slow temperature rates employed during EPR measurements with the NCSU VT. Indeed, dependence of the apparent van't Hoff enthalpy on the DSC temperature rate shown in Fig. 9B illustrates that extrapolation to zero rate is somewhat dependent upon which data points are selected. Finite time response of the calorimeter could also decrease the apparent cooperative unit number.

It should be noted here that slow temperature rates in DSC experiments are not always practical since the DSC signal decreases proportionally to both the temperature rate and the number of lipid molecules. Thus, for systems exhibiting slow phase transition kinetics the use of DSC could lead to some systematic errors in thermodynamic parameters. On the other hand, magnetic resonance experiments could always be carried out at conditions closely corresponding to thermodynamic equilibrium and, thus, should be free from temperature rate artifacts.

4. Conclusions

Here we demonstrate that variable temperate EPR experiments could be improved substantially by implementing the NCSU variable temperature accessory that features digital temperature control and high-efficiency radiators for heat exchange. The temperature stability of this new accessory after initial 15 min equilibration is about ± 0.007 K. For a standard 1-cm-long capillary sample arranged inside an EPR tube filled with silicon oil, the temperature variations do not exceed ± 0.033 K over the sample temperature range from 283 to 333 K. Such improvements demonstrate the advantages gained by utilizing the NCSU VT in studies of phospholipid bilayers and, specifically, phase transitions experiments with MLV that are known to occur within the 0.1–0.3 K temperature range.

The variable temperature accessory we described here does not require a fragile and expensive custom-made quartz dewars that many currently available systems would normally require. Our system is inexpensive, robust, and easy to assemble. More importantly, it could be used with any other EPR accessories and inserts such as flat cell for aqueous samples, multicapillary AquaX cell (Bruker), and tissue cells. The only drawback of our system is a small distortion of the magnetic field modulation field that is caused by placing conductive aluminum plates in the vicinity of the modulation coils.

With this new accessory, we have compared thermodynamic parameters of the gel-to-liquid phase transition of spin-labeled and unlabeled DMPC. It was demonstrated that when MLV DMPC was labeled with 5PC at 1 mol%, the phase transition temperatures from EPR and DSC agree within ± 0.02 K experimental error. For unlabeled MLV DMPC sample, DSC detected the same phase transition temperature. Furthermore, DSC indicated that the addition of 1 mol% decreases the cooperative unit number, N, of MLV

DMPC by only ≈14%. However, for the same spin-labeled sample EPR reported cooperative unit number $N = 676 \pm 36$, which is almost 50% higher than that obtained from DSC ($N = 458 \pm 18$). These high values of N indicate that 5PC are not excluded into domains that are different from the bulk lipid phase. Thus, the lipid domains should include at least several spin-labeled lipid molecules. Overall, this confirms ideal solution behavior for DMPC:5PC (100:1 mol ratio) mixtures for the bilayer in gel or liquid phases.

To summarize, our data provide DSC and EPR evidence that in studies of the gel-to-liquid phase transition the effect of bilayer perturbation by spin-labeled lipids is negligible and there is essentially no effect on the thermodynamic parameters of the transition. This resolves one of the long-standing concerns that spin labels even at low concentrations could perturb the bilayer at least locally and therefore would report somewhat different thermodynamic properties. This might serve as an indication that when molecules with structures similar to those of lipids such as 5PC are introduced at low concentrations, they are easily accommodated by fluid phospholipid bilayers without significant losses of the lipid cooperativity.

It further appears that in studies involving phase transition that require very slow temperatures rates, the use of spin-labeling EPR methods with a variable temperature accessory described here could be advantageous over DSC. One such example is substrate-supported and/or nanotube-confined bilayers that are known to have slower kinetics of lipid rearrangements than unsupported multilamellar vesicles [19].

Acknowledgments

This work was supported by the DOE Contract DE-FG02-02ER15354 to A.I.S. Acknowledgment is made to the Donors of the American Chemical Society Petroleum Research Fund, for partial support of this research through ACS PRF# 40232-G7 (to A.I.S). Instrumental facilities for this research were supported by NSF DMR-0114200 and NSF MRI-0420775 (to A.I.S.).

References

[1] A.I. Smirnov, R.B. Clarkson, R.L. Belford, EPR linewidth (T_2) method to measure oxygen permeability of phospholipid bilayers and its use to study the effects of low ethanol concentrations, J. Magn. Reson. B 111 (1996) 149–157.

[2] P.D. Morse II, R.L. Magin, H.M. Swartz, Improved temperature control for samples in electron-paramagnetic-resonance spectroscopy, Rev. Sci. Instrum. 56 (1985) 94–96.

[3] N. Albon, J.M. Sturtevant, Nature of the gel to liquid transition of synthetic phosphatidylcholines, Proc. Natl. Acad. Sci. USA 75 (1978) 2258–2260.

[4] D. Marsh, A. Watts, P.F. Knowles, Cooperativity of the phase transition in single- and multibilayer lipid vesicles, Biochim. Biophys. Acta 465 (1977) 500–514.

[5] S.-C. Chen, J.M. Sturtevant, K. Conklin, B.J. Gaffney, Calorimetric evidence for phase transitions in spin-labeled lipid bilayers, Biochemistry 21 (1982) 5096–5101.

[6] S.C. Chen, B.J. Gaffney, Paramagnetic resonance evidence for phase transitions in bilayers of pure spin labeled lipids, J. Magn. Reson. 29 (1978) 341–353.

[7] E.J. Shimshick, H.M. McConnell, Lateral phase separation in phospholipid membranes, Biochemistry 12 (1973) 2351–2360.

[8] A. Kusumi, W.K. Subczynski, J.S. Hyde, Oxygen transport parameter in membranes as deduced by saturation recovery measurements of spin–lattice relaxation times of spin labels, Proc. Natl. Acad. Sci. USA 79 (1982) 1854–1858.

[9] A.I. Smirnov, T.I. Smirnova, P.D. Morse II, Very high frequency electron paramagnetic resonance of 2,2,6,6-tetramethyl-1-piperidinyl-oxy in 1,2-dipalmitoyl-*sn*-glycero-3-phosphatidyl-choline liposomes: partitioning and molecular dynamics, Biophys. J. 68 (1995) 2350–2360.

[10] M.K. Jain, N.M. Wu, Effect of small molecules on the dipalmitoyl lecithin liposomal bilayer: III. Phase transition in lipid bilayer, J. Membr. Biol. 34 (1977) 157–201.

[11] A.D. Keith, M. Sharnoff, G.E. Cohn, A summary and evaluation of spin labels used as probes for biological membrane structure, Biochim. Biophys. Acta 300 (1973) 379–419.

[12] B.D. Ladbrooke, D. Chapman, Thermal analysis of lipids, proteins and biological membranes: a review and summary of some recent studies, Chem. Phys. Lipids 3 (1969) 304–356.

[13] R.D. Rataiczak, M.T. Jones, Investigation of the cw saturation technique for measurement of electron spin–lattice relaxation: application to the benzene anion radical, J. Chem. Phys. 56 (1972) 3898–3911.

[14] K.C. Cho, C.L. Choy, K. Young, Kinetics of the pretransition of synthetic phospholipids a calorimetric study, Biochim. Biophys. Acta 663 (1981) 14–21.

[15] B.R. Lentz, E. Freire, R.L. Biltonen, Fluorescence and calorimetric studies of phase transitions in phosphatidylcholine multilayers: kinetics of the pretransition, Biochemistry 17 (1978) 4475–4480.

[16] A.I. Smirnov, R.L. Belford, Rapid quantitation from inhomogeneously broadened EPR spectra by a fast convolution algorithm, J. Magn. Reson. A 113 (1995) 65–73.

[17] A.I. Smirnov, T.I. Smirnova, Convolution-based algorithm: from analysis of rotational dynamics to EPR oximetry and protein distance measurements, Biol. Magn. Reson. 21 (2004) 277–348.

[18] S. Mabrey, J.M. Sturtevant, Investigation of phase transitions of lipids and lipid mixtures by high sensitivity differential scanning calorimetry, Proc. Natl. Acad. Sci. USA 73 (1976) 3862–3866.

[19] A.M. Alaouie, A.I. Smirnov, Cooperativity and kinetics of phase transitions in nanopore-confined bilayers studied by differential scanning calorimetry, Biophys. J. 88 (2005) L11–L13.

[20] H. Heerklotz, J. Seelig, Application of pressure perturbation calorimetry to lipid bilayers, Biophys. J. 82 (2002) 1445–1452.

[21] J.M. Sturtevant, A scanning calorimetric study of small molecule–lipid bilayer mixtures, Proc. Natl. Acad. Sci. USA 79 (1982) 3963–3967.

[22] H. Trauble, E. Sackmann, Crystalline–liquid crystalline phase transition of lipid model membranes. III. Structure of a steroid–lecithin system below and above the lipid-phase transition, J. Am. Chem. Soc. 94 (1972) 4499–4510.